Substrate recognition and mechanism revealed by ligand-bound polyphosphate kinase 2 structures

Alice E. Parnell[a,1], Silja Mordhorst[b,1], Florian Kemper[c], Mariacarmela Giurrandino[a], Josh P. Prince[a], Nikola J. Schwarzer[c], Alexandre Hofer[d], Daniel Wohlwend[c], Henning J. Jessen[d,e], Stefan Gerhardt[c], Oliver Einsle[c,f], Petra C. F. Oyston[g,h], Jennifer N. Andexer[b,2], and Peter L. Roach[a,g,2]

[a]Chemistry, University of Southampton, Southampton, Hampshire SO17 1BJ, United Kingdom; [b]Institute of Pharmaceutical Sciences, Albert-Ludwigs-University Freiburg, 79104 Freiburg, Germany; [c]Institute of Biochemistry, Albert-Ludwigs-University Freiburg, 79104 Freiburg, Germany; [d]Organic Chemistry Institute, University of Zürich, 8057 Zürich, Switzerland; [e]Institute of Organic Chemistry, Albert-Ludwigs-University Freiburg, 79104 Freiburg, Germany; [f]Bioss Centre for Biological Signalling Studies, Albert-Ludwigs-University Freiburg, 79104 Freiburg, Germany; [g]Institute for Life Sciences, University of Southampton, Southampton, Hampshire SO17 1BJ, United Kingdom; and [h]Biomedical Sciences, Defence Science and Technology Laboratory Porton Down, SP4 0JQ Salisbury, United Kingdom

Edited by David Avram Sanders, Purdue University, West Lafayette, IN, and accepted by Editorial Board Member Gregory A. Petsko February 13, 2018 (received for review June 20, 2017)

Inorganic polyphosphate is a ubiquitous, linear biopolymer built of up to thousands of phosphate residues that are linked by energy-rich phosphoanhydride bonds. Polyphosphate kinases of the family 2 (PPK2) use polyphosphate to catalyze the reversible phosphorylation of nucleotide phosphates and are highly relevant as targets for new pharmaceutical compounds and as biocatalysts for cofactor regeneration. PPK2s can be classified based on their preference for nucleoside mono- or diphosphates or both. The detailed mechanism of PPK2s and the molecular basis for their substrate preference is unclear, which is mainly due to the lack of high-resolution structures with substrates or substrate analogs. Here, we report the structural analysis and comparison of a class I PPK2 (ADP-phosphorylating) and a class III PPK2 (AMP- and ADP-phosphorylating), both complexed with polyphosphate and/or nucleotide substrates. Together with complementary biochemical analyses, these define the molecular basis of nucleotide specificity and are consistent with a Mg^{2+} catalyzed in-line phosphoryl transfer mechanism. This mechanistic insight will guide the development of PPK2 inhibitors as potential antibacterials or genetically modified PPK2s that phosphorylate alternative substrates.

kinase | polyphosphate | enzyme structure | kinetics

Polyphosphate (polyP) is an inorganic linear polymer of tens to thousands of phosphoryl monomers and is found in all branches of life (1). The biological functions of polyP are numerous, including energy storage, metal chelation, buffering, DNA uptake, gene regulation, and the bacterial stringent response to nutrient deficiency (1, 2). Its importance in processes crucial for bacterial pathogens such as biofilm formation, persistence, motility, quorum sensing, and synthesis of virulence factors has made the enzymes involved in its biosynthesis and utilization promising targets for the development of new antibiotics (2–7). In nature, polyP is synthesized and degraded by polyphosphate kinases (PPKs) that catalyze the reversible transfer of the terminal phosphoryl residue from nucleoside 5′-triphosphates to polyP. Two large, structurally unrelated families of bacterial PPKs have been characterized so far: PPK1 enzymes that favor polyP synthesis (3, 8) and the PPK2 family that favors nucleotide phosphorylation. PPK2s can be phylogenetically subdivided into three classes (9): class I preferentially phosphorylates nucleoside diphosphates (10–12), class II converts nucleoside monophosphates into diphosphates (11, 13–15), and class III can phosphorylate either nucleoside mono- or diphosphates (9) (Fig. 1*A*). A small subgroup of PPKs that favors the phosphorylation of pyrimidine nucleobases instead of purine nucleobases, which has been designated as PPK3, clusters phylogenetically with the PPK2 family (class I) (16).

The structure and mechanism of the PPK1 enzyme from *Escherichia coli* are well characterized (3, 17). Although not a genuine membrane enzyme, PPK1 seems to be associated with the membrane (18), which makes the purification process difficult. The mechanism is proposed to proceed via a phosphorylated enzyme intermediate (8), which is supported by a crystal structure with β,γ-imidoadenosine 5′-triphosphate (AMPPNP) bound in the active site [Protein Data Bank (PDB) ID code 1XDP] (3). In a few cases, PPK1 has been used as a catalyst for ATP regeneration, e.g., as so-called "energy beads" in the form of active inclusion bodies (19). Due to their preference for nucleotide phosphorylation, PPK2 enzymes are more often used for ATP, or—in the case of PPK2 classes II and III—ADP regeneration (20–24); in addition, they are generally easier to purify, as they are soluble cytoplasmic enzymes (25).

Several bacterial PPK2s have been structurally characterized, including the class I enzymes from *Sinorhizobium meliloti* (PDB ID code 3CZQ) (11) and *Francisella tularensis* (PDB ID code 4YEG) (26), the class II enzyme from *Pseudomonas aeruginosa* (PDB ID code 3CZP) (11), and the class III enzyme (9) from

Significance

Polyphosphate kinases (PPKs) are involved in many metabolic processes in bacteria, including pathogenic species. As these enzymes are not present in animals, they are a prime target for the development of novel antibiotics. The detailed knowledge of the mechanism of action and structure–function relationships of these enzymes is of utmost importance for the identification and design of new pharmaceutically active compounds and the rational improvement of lead structures. In addition, PPKs use inexpensive and stable polyphosphate as a phosphate donor and phosphorylate nucleoside 5′-mono- as well as 5′-diphosphates. This makes them of special interest for application in ATP regeneration systems, which can be efficiently coupled to ATP-consuming enzymes in environmentally friendly and sustainable biotechnological processes.

Author contributions: A.E.P., S.M., M.G., D.W., H.J.J., O.E., P.C.F.O., J.N.A., and P.L.R. designed research; A.E.P., S.M., F.K., M.G., J.P.P., N.J.S., A.H., D.W., S.G., O.E., J.N.A., and P.L.R. performed research; A.E.P., S.M., F.K., M.G., J.P.P., N.J.S., A.H., D.W., H.J.J., S.G., O.E., P.C.F.O., J.N.A., and P.L.R. analyzed data; and A.E.P., S.M., J.P.P., H.J.J., O.E., P.C.F.O., J.N.A., and P.L.R. wrote the paper.

The authors declare no conflict of interest.

This article is a PNAS Direct Submission. D.A.S. is a guest editor invited by the Editorial Board.

Data deposition: The atomic coordinates and structure factors have been deposited in the Protein Data Bank, www.wwpdb.org (PDB ID codes 5LC9, 5LCD, 5LDB, 5LD1, 5MAQ, 5LL0, 5LLB, 5LLF, 5O6K, and 5O6M).

[1]A.E.P. and S.M. contributed equally to this work.

[2]To whom correspondence may be addressed. Email: jennifer.andexer@pharmazie.uni-freiburg.de or plr2@soton.ac.uk.

This article contains supporting information online at www.pnas.org/lookup/suppl/doi:10.1073/pnas.1710741115/-/DCSupplemental.

Published online March 12, 2018.

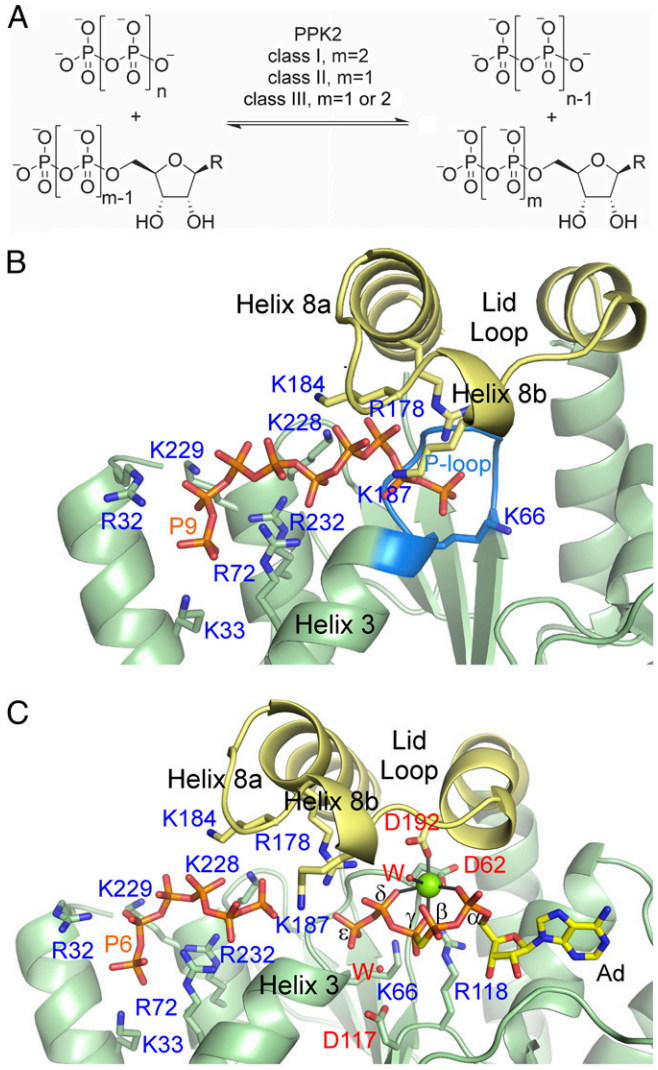

Fig. 1. PPK2 catalysis and substrate binding. (*A*) Phosphotransfer reactions catalyzed by PPK2 classes. R, nucleobase. (*B*) PolyP binding to *Ft*PPK2. The lid loop is shown in yellow and the Walker A motif (P-loop) is shown in blue. P9, nonaphosphate. (*C*) Active-site region of the *Ft*PPK2:AMPPCPPP:polyP complex. The lid loop is shown in yellow. Ad, adenine moiety; P6, hexaphosphate; W, water.

Arthrobacter aurescens (PDB ID code 3RHF). However, the absence of substrate-bound structures has made rationalization of the PPK2 mechanism and substrate specificity difficult (9). Here we compare different enzyme-ligand complexes of a class I PPK2 and a class III PPK2. Combining thermodynamic and kinetic analyses with these structures, we propose a model for substrate binding and discrimination as well as a mechanism for PPK2s.

Results

Three-Dimensional Structures. We report here the crystal structure of *Meiothermus ruber* (*Mr*) PPK2 as the archetypal class III PPK2 (9) to a resolution of 1.90 Å. The overall structure is consistent with the general PPK2 fold as described for other class I and II PPK2s (9, 11), which belong to the family of the P-loop kinases and typically contain two conserved sequence motifs (Walker A and Walker B, phosphate-binding loops) and a flexible lid loop built of two α-helices (*SI Appendix*, Fig. S1). *Mr*PPK2 forms a crystallographic tetramer; each protomer consists of a five-stranded parallel β-sheet surrounded by 10 α-helices. There is a high degree of similarity between the overall structure of *Mr*PPK2 and the previously reported PPK2 structures (26) (*SI Appendix*, Table S2), the closest being that of the class III *A. aurescens* enzyme (PDB ID code 3RHF) with an rmsd of 1.3 Å over 268 residues, compared with the class I *F. tularensis* (*Ft*) (PDB ID code 5LLB) structure with an rmsd of 1.5 Å over 239 aligned residues.

To gain insight into the substrate-binding mode of PPK2 enzymes, *Ft*PPK2 was cocrystallized with polyP, revealing nine phosphoryl residues bound in a channel between helix 3 of the protein core and helix 8a of the lid loop (Fig. 1*B*). The polyP is precisely positioned by a constellation of positively charged residues, many of which are conserved across all PPK2s (*SI Appendix*, Fig. S1), and two phosphoryl residues are juxtaposed to the catalytically important P-loop (Walker A motif, Fig. 1*B*). This polyP channel is conserved in all of the available PPK2 structures including *Mr*PPK2, and a similar structural feature has been described for PPK1 enzymes (3).

In the absence of reported nucleotide-bound PPK2 structures, the question remained how this polyP channel connects to the active site and how each class of PPK2 recognizes its particular nucleotide(s). To address this, we determined additional structures with nucleotide ligands. Cocrystallization of *Ft*PPK2 with polyP and the nonhydrolyzable ATP analog β,γ-methylene adenosine

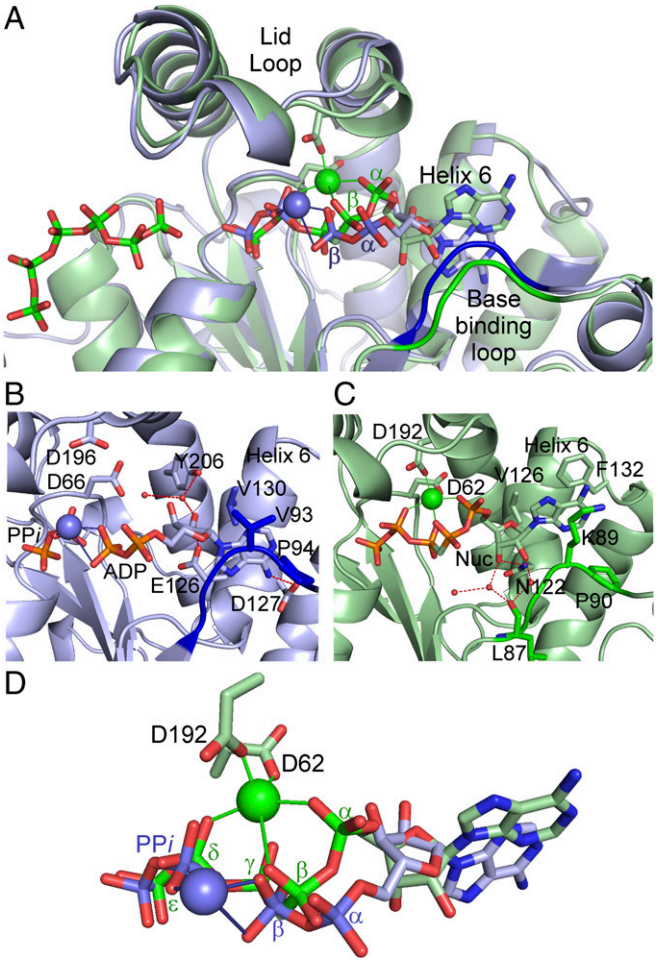

Fig. 2. PPK2 nucleotide-binding. (*A*) Overlay of *Mr*PPK2:ADP:PP_i complex (blue) with the *Ft*PPK2:AMPPCPPP:polyP complex (green). (*B*) Detail of nucleotide interactions for *Mr*PPK2. (*C*) Detail of nucleotide interactions for *Ft*PPK2. Magnesium ions shown as larger spheres, water molecules as smaller red spheres. Nuc, AMPPCPPP nucleotide. (*D*) Overlay of bound nucleotide conformations derived from the *Mr*PPK2:ADP:PP_i complex (blue) and the *Ft*PPK2:AMPPCPPP:polyP complex (green).

Table 1. Biochemical characterization of wild-type and variant PPK2s

Protein		Nucleotide turnover*				PolyP binding		
Source	Variant	k_{cat} ($\times 10^{-1}\cdot s^{-1}$)	K_M (mM)	R^2	k_{cat}/K_M ($\mu M\cdot s^{-1}$)	K_d (μM)	ΔG (kcal·mol^{-1})†	Binding stoichiometry
Ft	WT	31.7 ± 2.20‡	0.546 ± 0.079‡	0.99‡	5,788‡	0.62 ± 0.19	−8.52 ± 0.32	0.67 ± 0.05
Mr	WT	70.7 ± 3.86§	0.033 ± 0.009§	0.93	214,242	ND	ND	ND
		2.46 ± 0.08¶	0.246 ± 0.027¶	0.99	100,000	ND	ND	ND
Ft	D62A	0.159 ± 0.018	2.47 ± 0.746	0.91	6.43	ND	ND	ND
Ft	D117N	0.724 ± 0.047	4.03 ± 0.532	0.99	18.0	0.47 ± 0.03	−8.74 ± 0.04	0.40 ± 0.04
Mr	N121D	24.9 ± 0.82§	0.075 ± 0.010§	0.98	33,200	ND	ND	ND
		0.147 ± 0.008¶	0.358 ± 0.065¶	0.97	4,106	ND	ND	ND
Ft	D192A	0.015 ± 0.002	3.21 ± 0.870	0.94	0.47	ND	ND	ND
Ft	K66A	0.053 ± 0.008	12.3 ± 4.12	0.96	0.44	3.58 ± 0.80	−7.46 ± 0.12	0.43 ± 0.01
Ft	R118A	0.022 ± 0.07	6.18 ± 3.54	0.83	0.37	0.98 ± 0.10	−8.20 ± 0.06	0.60 ± 0.01
Ft	R178A	0.031 ± 0.004	3.25 ± 1.05	0.92	0.95	7.50 ± 0.20	−7.00 ± 0.20	0.69 ± 0.07

ND, not determined; WT, wild type.
*Kinetic parameters were determined by HPLC analysis of initial rates of product formation. All rates for *Ft*PPK2 were measured for phosphorylation of ADP.
†Calculated at 20 °C.
‡Data taken from Batten et al. (26).
§For phosphorylation of AMP.
¶For phosphorylation of ADP.

5′-triphosphate (AMPPCP) gave a structure featuring a Mg^{2+} bound by the active site residues Asp62^{FtPPK2} (Asp66^{MrPPK2}, Walker A motif) and Asp192^{FtPPK2} (Asp196^{MrPPK2}, lid loop, Fig. 1*C* and *SI Appendix*, Fig. S2*C*). The electron density map (*SI Appendix*, Fig. S3*A*) clearly indicates that, during the crystallization, two additional phosphoryl units have been transferred onto the terminus of AMPPCP, yielding β,γ-methylene adenosine 5′-pentaphosphate (AMPPCPPP). Oxygens of the α-, γ-, and δ-phosphoryl groups occupy three ligand sites around the magnesium ion (Fig. 1*C* and *SI Appendix*, Fig. S2*C*). The remaining Mg^{2+} ligand is poorly resolved and modeled as a water. The complete conservation of the aspartyl residues throughout all PPK2 classes (*SI Appendix*, Fig. S1) and the octahedral coordination pattern led us to hypothesize that this is the native position of the Mg^{2+} during catalysis. Beyond the ε-phosphate position of the nucleotide ligand in the *Ft*PPK2-AMPPCPPP structure, there is a short break (~7.0 Å) in the electron density and then further density traverses the polyP binding channel, consistent with the binding of six more phosphoryl residues (Fig. 1*C*, P6). Interactions of the lid loop region with the two substrates and the active-site Mg^{2+} closes the lid loop by an ~4.5-Å movement of helix 8b (in comparison with the unliganded structure). The PPK1 catalyzed transfer of pyrophosphate to GDP to form G4P has been reported (27), but efforts to detect *Ft*PPK2 catalyzed formation of AMPPCPPP in free solution (as opposed to in crystals) were unsuccessful.

Soaking *Mr*PPK2 crystals with the substrates AMP, ADP, ATP, and the transition state mimic adenosine 5′-pentaphosphate (A5P) resulted in a series of nucleotide-bound structures (Fig. 2 and *SI Appendix*, Table S1). Soaking with A5P resulted in a structure of *Mr*PPK2 with ADP and pyrophosphate (PP_i) bound at the active site. Some of these structures revealed Mg^{2+}, coordinated either by the active-site Asp residues (Asp66^{MrPPK2}, Walker A motif, and Asp196^{MrPPK2}, lid loop) and/or at alternative positions (e.g., Fig. 2*B*), predominantly bound to nucleoside phosphates. For *Mr*PPK2, a structure containing an intact polyP chain could not be solved, but the corresponding polyP-binding channel is delineated by a series of individual phosphate ions observed in the structure of the *Mr*PPK2 Asn121Asp variant soaked with ATP (*SI Appendix*, Fig. S2*B*).

Comparing *Mr*PPK2 and *Ft*PPK2 nucleotide-bound structures (Fig. 2 and *SI Appendix*, Fig. S4), the nucleoside moiety is sandwiched in a pocket between a base-binding loop (residues 87–90^{FtPPK2}/91–94^{MrPPK2}) and helix 6. In *Mr*PPK2 (Fig. 2*B*), this pocket includes hydrophobic interactions from Val93^{MrPPK2} and Pro94^{MrPPK2} from the base-binding loop and Val130^{MrPPK2} from helix 6. In *Ft*PPK2, interactions come from pi-stacking the purine against Phe132^{FtPPK2} and hydrophobic interactions from Lys89^{FtPPK2} and Pro90^{FtPPK2} from the base-binding loop (Fig. 2*C*). Other interactions contribute to the orientation of the nucleoside moieties: in *Mr*PPK2, the adenine 6-amino group forms a hydrogen bond with Asp127^{MrPPK2} and the ribose 2′-hydroxyl hydrogen bonds to Glu126^{MrPPK2} and via a water to Tyr206^{MrPPK2}; in *Ft*PPK2, the ribose interacts with Asn122^{FtPPK2} via a hydrogen-bonding network (9). Some nucleotide-binding residues are conserved across PPK2 subclasses (*SI Appendix*, Figs. S1 and S4), but interpretation of sequence conservation over multiple PPK2 subclasses is complicated by the different phosphorylation states of the preferred nucleotide substrates that enforce alternative interactions on the conserved residues. Between the *Mr*PPK2 and *Ft*PPK2 structures, this results in different binding modes for the nucleoside moieties that adopt "flipped" orientations relative to each other (Fig. 2 *A* and *D*). Compared with *Ft*PPK2, the flipped conformation of the adenosine moiety shifts the *Mr*PPK2 base-binding pocket ~4.5 Å deeper into the protein. A structural overlay of *Mr*PPK2 and *Ft*PPK2 (Fig. 2*A*) shows that the different nucleotide conformations (Fig. 2*D*) result in the α-phosphate of AMP in *Mr*PPK2 and the β-phosphate of the nucleotide substrate in *Ft*PPK2 occupying similar positions (~1.6 Å apart) relative to the presumed catalytic Mg^{2+}-binding site in *Ft*PPK2. We hypothesize that the functional importance of fine-tuning the nucleotide-binding site is to position the nucleophilic phosphate on an ideal trajectory for nucleophilic attack of the polyP terminal residue.

The structures of *Mr*PPK2 complexed with nucleotides (AMP, ADP, ATP, and ADP plus PP_i) show them bound in very similar positions and conformations. In the wild-type *Mr*PPK2:ATP complex, but not in the corresponding structure of the Asn121Asp variant, a second equivalent of ATP is bound near the active site (*SI Appendix*, Fig. S3*C*). The two triphosphate chains are bound to Mg^{2+}, and while the first ATP is bound to the active site in a similar manner to the AMP and ADP structures, the adenosine moiety of the second ATP protrudes from the active site (*SI Appendix*, Fig. S3 *C* and *D*), making contacts with the neighboring protomer. The residues contacting the second ATP are not well conserved in *Ft*PPK2 or other PPK2s and the physiological relevance of the second equivalent of ATP is unclear, but the hypothesis of ATP-mediated regulation is under investigation.

Nevertheless, as there is no polyP chain bound in these structures, there remains a degree of uncertainty as to how *Mr*PPK2 precisely positions the nucleotide to achieve two phosphorylation

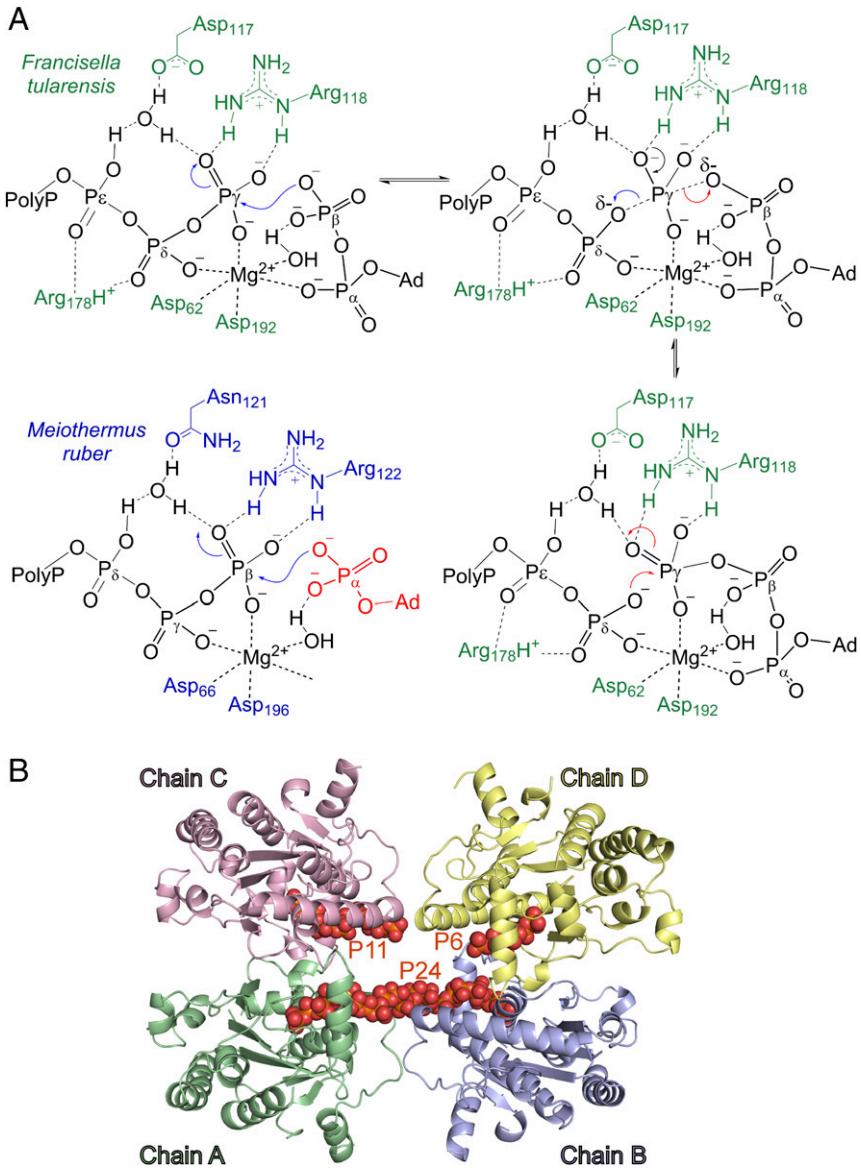

Fig. 3. PPK2 mechanism and interaction with polyP. (*A*) Proposed mechanism of *Ft*PPK2 and the modified nucleotide-binding mode for *Mr*PPK2 that permits phosphorylation of the α-phosphate (highlighted in red). Blue curly arrows indicate the forward reaction (ATP formation), red curly arrows the reverse reaction, and black curly arrows are common to both. (*B*) Structure of *Ft*PPK2 Asp117Asn variant cocrystallized with polyP. Labels indicate the polyP lengths: P6, P11, and P24.

steps: in addition to catalyzing the phosphorylation of AMP, *Mr*PPK2 also catalyzes the conversion of ADP to ATP, but at a reduced rate (Table 1 and *SI Appendix*, Figs. S5 and S6). For *Mr*PPK2 catalysis in the direction of nucleotide phosphorylation, a relatively small conformational adjustment of the 5′-substituent (either phosphate or diphosphate) positions the terminal phosphate on a favored trajectory for nucleophilic attack on the polyP, possibly with the assistance of an active-site bound Mg^{2+}.

Oligomerization of PPK2s in Solution. In the crystalline state, both *Ft* and *Mr*PPK2s are tetrameric. Oligomerization of PPK2s in the functionally important solution state was determined using a combination of size exclusion chromatography and right-angle light scattering (RALS) (*SI Appendix*, Figs. S7–S9). This showed that *Ft*PPK2 behaves as a monomer in the absence of substrate, but addition of polyP promoted dimerization. In the absence of substrates, *Mr*PPK2 is trimeric in solution, but forms tetramers in the presence of polyP, which in turn form higher multimers of the tetrameric form (i.e., containing 8, 12, and 16 protomers). We hypothesize that the polyP (25 residues average length) is sufficiently long to bridge between the protomer active sites, inducing the formation of the observed higher oligomers (*SI Appendix*, Fig. S10).

Activity and PolyP Binding of Sequence Variants. To complement the structural studies, the PPK2 wild types and several sequence variants were analyzed for activity (*SI Appendix*, Figs. S5, S6, and S11), and the polyP dissociation constant was determined using isothermal calorimetry (ITC) (Table 1). As expected, Lys66Ala$^{Ft\text{PPK2}}$ (Walker A motif) and Arg178Ala$^{Ft\text{PPK2}}$ (lid loop) showed weaker polyP binding and slower turnover relative to the wild-type enzyme. *Ft*PPK2 Asp117 and *Mr*PPK2 Asn121 occupy equivalent positions in the structures and to probe the functional significance of this difference, the variant Asp117Asn$^{Ft\text{PPK2}}$ was prepared. Asp117Asn$^{Ft\text{PPK2}}$ shows a decreased k_{cat}, but as expected, polyP binding is unaffected; the reciprocal *Mr*PPK2 variant (Asn121Asp$^{Mr\text{PPK2}}$) also shows decreased activity. Both variants were crystallized to analyze the effect of the mutation on the active site. The overall

structures as well as the active sites are very similar with rmsds for C_α atoms of 0.394 Å and 0.557 Å for *Ft*PPK2 and *Mr*PPK2, respectively. As described above, soaking Asn121Asp^{MrPPK2} with ATP resulted in a structure with the nucleotide bound in the same manner as the wild-type ATP complex. The structure of the Asp117Asn^{FtPPK2} variant cocrystallized with polyP (average length 25) revealed a 24-mer polyP stretching between protomers A and B (Fig. 3*B*). This structure may explain the polyP/*Ft*PPK2-binding stoichiometry of ∼0.5 observed by ITC (Table 1) and provides a mechanistic rationale for the formation of higher multimers observed in the RALS experiments (*SI Appendix*, Figs. S7–S10). Consistent with its proposed role, Arg118Ala^{FtPPK2} (Walker B motif) showed little or no effect on the K_d for polyP, and in the structures this arginine makes contacts only with the nucleotide phosphates.

Discussion

Different mechanisms leading to the AMPPCPPP complex with *Ft*PPK2 can be envisaged; in one scenario, diphosphate transfer arises from the nucleophilic attack of AMPPCP on the terminal residue of polyP forming a cross-linked intermediate, followed by hydrolysis of the P_ε-O-P_ζ link under crystallization conditions (*SI Appendix*, Fig. S12). Soaking A5P into *Mr*PPK2 crystals also resulted in a chemical reaction: the electron density is consistent with bound ADP and PP_i ligands, likely derived from A5P. The overlay of *Ft*PPK2:AMPPCPPP:$PolyP_6$ with *Mr*PPK2:ADP:PP_i (Fig. 2*A*) or with *Mr*PPK2-N121D:ATP:P_i (*SI Appendix*, Fig. S2*B*) clearly identifies the course of the polyP-binding channel, which passes under the lid loop to the nucleotide-binding site.

Comparison of the ligand-bound *Mr* and *Ft*PPK2 structures with the unliganded PPK2 structures present in the Protein Data Bank using DALI (28) showed (*SI Appendix*, Table S2) the highest degree of similarity between the class I enzymes (*Ft* and *S. meliloti*, rmsd 0.9 Å over 249 residues) and the class III enzymes (*Mr* and *A. aurescens*, rmsd 1.3 Å over 268 residues). The class II *P. aeruginosa* PPK2 catalytic domain shows less similarity to either ligand-bound structure (rmsd 1.7 Å to *Mr* over 249 residues and 1.7 Å to *Ft* over 241 residues).

The nucleotide-binding site of exclusively AMP-phosphorylating class II PPK2s may be inferred from residues functionally conserved in both classes I and II that participate in enzyme–nucleotide interactions. Characteristic for class I PPK2s is the pi-stacking interaction of the adenine base with Phe132^{FtPPK2}; this residue is conserved in PPK2 classes I and II, but not in class III, and suggests that other class I PPK2s and class II PPK2s bind the nucleotide purine and ribose in a similar manner to *Ft*PPK2 (*SI Appendix*, Fig. S1). In contrast, *Mr*PPK2 recognizes the adenine amino group through interactions with Asp127^{MrPPK2}, which is conserved solely in class III PPK2s; it is replaced in class I and II PPK2s (*SI Appendix*, Fig. S1) with an arginine residue, the side chain of which is directed away from the active site. Class III PPK2s have been proposed to be phylogenetically closest to a PPK2 ancestor (9), but the radically different conformations of the ribose moiety observed in nucleotide-bound complexes of *Ft* and *Mr*PPK2s (Fig. 2*D*) emphasize the evolutionary divergence required to accommodate nucleotide substrates in different phosphorylation states (i.e., either AMP or ADP).

Understanding the mechanism of phosphoryl transfer reactions is a long-standing and important biochemical problem (29, 30). Evidence from a range of techniques (31), including linear free-energy relationships and kinetic isotope effects (32), have led to the tentative conclusion that, during substitution at a singly substituted phosphate (such as the γ-phosphate of ATP), the reaction likely proceeds via a "loose" transition state with a small degree of bond formation from the incoming nucleophile and a large degree of bond cleavage to the leaving group (29). Our proposed mechanism for PPK2s (Fig. 3*A*) features the in-line nucleophilic attack of the nucleotide on polyP that is activated by binding to the active-site Lewis acidic Mg^{2+} ion. Arg178^{FtPPK2}/Arg182^{MrPPK2} from the lid loop orients the polyP chain in the active site. In *Ft*PPK2, ADP coordinated to the Mg^{2+} via the α-phosphate may allow nucleophilic attack by the β-phosphate, which is not directly coordinated with Mg^{2+}, on the terminal phosphorus of polyP (Fig. 3*A*). Analogously, during *Mr*PPK2-catalyzed formation of ADP from AMP, the alternate flipped conformation of the adenosine positions the α-phosphate in the nucleophilic site. Formation of a trigonal bipyramidal transition state may be stabilized by hydrogen-bonding to a water molecule coordinated by Asp117^{FtPPK2}/Asn121^{MrPPK2} (Figs. 1*C* and 3*A*); alternatively, this Asx-water pair may protonate and thus stabilize this structure. Collapse of the transition state yields $polyP_{n-1}$ and ATP or ADP for *Ft*PPK2 or *Mr*PPK2, respectively. The proximal polyP residue (Fig. 1*B*) lies between the P-loop (Walker A motif) and Lys66^{FtPPK2}/Lys70^{MrPPK2}, which likely stabilizes the transition state by hydrogen-bonding to (or possibly by protonating) leaving groups (33, 34). Arg118^{FtPPK2}/Arg122^{MrPPK2} hydrogen-bonds to the γ-phosphate position in *Ft*PPK2, which may polarize the P-O bonds, increasing the electrophilicity of this phosphate in the direction of triphosphate synthesis. This mechanism resembles that developed for thymidylate kinase (34, 35), a close structural relative of the bacterial PPK2s (*SI Appendix*, Fig. S13) (36).

In conclusion, the importance of polyP metabolism for the virulence of bacterial pathogens (1, 5) has led to its proposal as a potential target for antibacterial discovery (37). The phosphorylation of a variety of (nucleotide) substrates driven by inexpensive and plentiful polyP leading to nucleoside di- and triphosphates has numerous prospective biotechnological applications (22–24, 38), and not only as biocatalysts for ATP regeneration systems. The mechanisms of catalysis and substrate selectivity described here provide a useful foundation for progress in both these areas.

Materials and Methods

Detailed synthetic procedures for the preparation of nucleotides and analogs, the expression and purification of wild-type and variant PPK2 proteins, and biochemical studies are described in *SI Appendix, SI Materials and Methods*. Purified PPK2 proteins were crystallized using the vapor diffusion method. Substrates and analogs were introduced either by cocrystallization or soaking, and structures were determined by X-ray diffraction experiments, model building, and refinement as detailed in *SI Appendix, SI Materials and Methods*.

ACKNOWLEDGMENTS. We thank Diamond Light Source for access to beamlines i24, i04, and i04-1 under proposal mx8889 and the staff of the Swiss Light Source for their support. This work was supported by funds from the US Defense Threat Reduction Agency Grant HDTRA1-11-1-0007; Defence Science and Technology Laboratory Grant DSTLX1000097311; Engineering and Physical Sciences Research Council Grant EP/M507623/1; Human Frontiers of Science Program Grant RGP0025/2016; and Deutsche Forschungsgemeinschaft Grant RTG1976.

1. Brown MR, Kornberg A (2004) Inorganic polyphosphate in the origin and survival of species. *Proc Natl Acad Sci USA* 101:16085–16087.
2. Rao NN, Gómez-García MR, Kornberg A (2009) Inorganic polyphosphate: Essential for growth and survival. *Annu Rev Biochem* 78:605–647.
3. Zhu Y, Huang W, Lee SS, Xu W (2005) Crystal structure of a polyphosphate kinase and its implications for polyphosphate synthesis. *EMBO Rep* 6:681–687.
4. Achbergerová L, Nahálka J (2011) Polyphosphate: An ancient energy source and active metabolic regulator. *Microb Cell Fact* 10:63.
5. Gerdes K, Maisonneuve E (2012) Bacterial persistence and toxin-antitoxin loci. *Annu Rev Microbiol* 66:103–123.
6. Shum KT, et al. (2011) Aptamer-mediated inhibition of Mycobacterium tuberculosis polyphosphate kinase 2. *Biochemistry* 50:3261–3271.
7. Chuang YM, Belchis DA, Karakousis PC (2013) The polyphosphate kinase gene ppk2 is required for Mycobacterium tuberculosis inorganic polyphosphate regulation and virulence. *MBio* 4:e00039-13.
8. Ahn K, Kornberg A (1990) Polyphosphate kinase from Escherichia coli. Purification and demonstration of a phosphoenzyme intermediate. *J Biol Chem* 265:11734–11739.
9. Motomura K, et al. (2014) A new subfamily of polyphosphate kinase 2 (class III PPK2) catalyzes both nucleoside monophosphate phosphorylation and nucleoside diphosphate phosphorylation. *Appl Environ Microbiol* 80:2602–2608.

10. Ishige K, Zhang H, Kornberg A (2002) Polyphosphate kinase (PPK2), a potent, polyphosphate-driven generator of GTP. *Proc Natl Acad Sci USA* 99:16684–16688.
11. Nocek B, et al. (2008) Polyphosphate-dependent synthesis of ATP and ADP by the family-2 polyphosphate kinases in bacteria. *Proc Natl Acad Sci USA* 105:17730–17735.
12. Lindner SN, Vidaurre D, Willbold S, Schoberth SM, Wendisch VF (2007) NCgl2620 encodes a class II polyphosphate kinase in Corynebacterium glutamicum. *Appl Environ Microbiol* 73:5026–5033.
13. Shi X, Rao NN, Kornberg A (2004) Inorganic polyphosphate in Bacillus cereus: Motility, biofilm formation, and sporulation. *Proc Natl Acad Sci USA* 101:17061–17065.
14. Zhang H, Rao NN, Shiba T, Kornberg A (2005) Inorganic polyphosphate in the social life of Myxococcus xanthus: Motility, development, and predation. *Proc Natl Acad Sci USA* 102:13416–13420.
15. Bonting CF, Kortstee GJ, Zehnder AJ (1991) Properties of polyphosphate: AMP phosphotransferase of Acinetobacter strain 210A. *J Bacteriol* 173:6484–6488.
16. Nahálka J, Pätoprstý V (2009) Enzymatic synthesis of sialylation substrates powered by a novel polyphosphate kinase (PPK3). *Org Biomol Chem* 7:1778–1780.
17. Kumble KD, Ahn K, Kornberg A (1996) Phosphohistidyl active sites in polyphosphate kinase of Escherichia coli. *Proc Natl Acad Sci USA* 93:14391–14395.
18. Akiyama M, Crooke E, Kornberg A (1992) The polyphosphate kinase gene of Escherichia coli. Isolation and sequence of the ppk gene and membrane location of the protein. *J Biol Chem* 267:22556–22561.
19. Nahálka J, Gemeiner P, Bucko M, Wang PG (2006) Bioenergy beads: A tool for regeneration of ATP/NTP in biocatalytic synthesis. *Artif Cells Blood Substit Immobil Biotechnol* 34:515–521.
20. Resnick SM, Zehnder AJ (2000) In vitro ATP regeneration from polyphosphate and AMP by polyphosphate:AMP phosphotransferase and adenylate kinase from Acinetobacter johnsonii 210A. *Appl Environ Microbiol* 66:2045–2051.
21. Kameda A, et al. (2001) A novel ATP regeneration system using polyphosphate-AMP phosphotransferase and polyphosphate kinase. *J Biosci Bioeng* 91:557–563.
22. Kulmer ST, Gutmann A, Lemmerer M, Nidetzky B (2017) Biocatalytic cascade of polyphosphate kinase and sucrose synthase for synthesis of nucleotide-activated derivatives of glucose. *Adv Synth Catal* 359:292–301.
23. Schwander T, Schada von Borzyskowski L, Burgener S, Cortina NS, Erb TJ (2016) A synthetic pathway for the fixation of carbon dioxide in vitro. *Science* 354:900–904.
24. Mordhorst S, Siegrist J, Müller M, Richter M, Andexer JN (2017) Catalytic alkylation using a cyclic S-adenosylmethionine regeneration system. *Angew Chem Int Ed* 56: 4037–4041.
25. Zhang H, Ishige K, Kornberg A (2002) A polyphosphate kinase (PPK2) widely conserved in bacteria. *Proc Natl Acad Sci USA* 99:16678–16683.
26. Batten LE, et al. (2015) Biochemical and structural characterization of polyphosphate kinase 2 from the intracellular pathogen Francisella tularensis. *Biosci Rep* 36:e00294.
27. Kuroda A, Kornberg A (1997) Polyphosphate kinase as a nucleoside diphosphate kinase in Escherichia coli and Pseudomonas aeruginosa. *Proc Natl Acad Sci USA* 94: 439–442.
28. Holm L, Rosenström P (2010) Dali server: Conservation mapping in 3D. *Nucleic Acids Res* 38:W545–W549.
29. Lassila JK, Zalatan JG, Herschlag D (2011) Biological phosphoryl-transfer reactions: Understanding mechanism and catalysis. *Annu Rev Biochem* 80:669–702.
30. Kirby AJ, Nome F (2015) Fundamentals of phosphate transfer. *Acc Chem Res* 48: 1806–1814.
31. Stockbridge RB, Wolfenden R (2009) The intrinsic reactivity of ATP and the catalytic proficiencies of kinases acting on glucose, N-acetylgalactosamine, and homoserine: A thermodynamic analysis. *J Biol Chem* 284:22747–22757.
32. Cleland WW, Hengge AC (2006) Enzymatic mechanisms of phosphate and sulfate transfer. *Chem Rev* 106:3252–3278.
33. Reinstein J, Schlichting I, Wittinghofer A (1990) Structurally and catalytically important residues in the phosphate binding loop of adenylate kinase of Escherichia coli. *Biochemistry* 29:7451–7459.
34. Ostermann N, et al. (2000) Insights into the phosphoryltransfer mechanism of human thymidylate kinase gained from crystal structures of enzyme complexes along the reaction coordinate. *Structure* 8:629–642.
35. Gardberg A, Shuvalova L, Monnerjahn C, Konrad M, Lavie A (2003) Structural basis for the dual thymidine and thymidylate kinase activity of herpes thymidine kinases. *Structure* 11:1265–1277.
36. Leipe DD, Koonin EV, Aravind L (2003) Evolution and classification of P-loop kinases and related proteins. *J Mol Biol* 333:781–815.
37. Singh M, et al. (2016) Establishing virulence associated polyphosphate kinase 2 as a drug target for Mycobacterium tuberculosis. *Sci Rep* 6:26900.
38. Andexer JN, Richter M (2015) Emerging enzymes for ATP regeneration in biocatalytic processes. *ChemBioChem* 16:380–386.